Femtosecond Laser Ablation Multicollector ICPMS Analysis of Uranium Isotopes in NIST Glass

Journal:	*Journal of Analytical Atomic Spectrometry*
Manuscript ID:	JA-ART-11-2014-000452.R1
Article Type:	Paper
Date Submitted by the Author:	24-Dec-2014

Complete List of Authors:	Duffin, Andrew; Pacific Northwest National Laboratory, Springer, Kellen; Pacific Northwest National Laboratory, Ward, Jesse; Pacific Northwest National Laboratory, Jarman, Kenneth; Pacific Northwest National Laboratory, Robinson, John; Pacific Northwest National Laboratory, Endres, Mackenzie; Pacific Northwest National Laboratory, Hart, Garret; Pacific Northwest National Laboratory, Gonzalez, Jhanis; L. Berkeley National Lab, EETD; Applied Spectra, Oropeza, Dayana; L. Berkeley National Lab, EETD Russo, R; Lawrence Berkeley National Lab, Willingham, David; Pacific Northwest National Laboratory, Naes, Benjamin; Pacific Northwest National Laboratory, Fahey, Albert; Naval Research Laboratory, ; Pacific Northwest National Laboratory, Eiden, Gregory; Pacific Northwest National Laboratory,

1.1.1 Title

Femtosecond Laser Ablation Multicollector ICPMS Analysis of Uranium Isotopes in NIST Glass

1.1.2 Author names

Andrew M. Duffin, Kellen W. Springer, Jesse D. Ward, Kenneth D. Jarman, John W. Robinson, Mackenzie C. Endres, Garret L. Hart, Jhanis J. Gonzales, Dayana Oropeza, Richard E. Russo, David G. Willingham, Benjamin E. Naes, Albert J. Fahey, Gregory. C. Eiden

1.1.3 Table of contents entry

1.1.4 Abstract

We utilized femtosecond laser ablation together with multi-collector inductively coupled plasma mass spectrometry to measure the uranium isotopic content of NIST 61x (x=0,2,4,6) glasses. The uranium content of these glasses is a linear two-component mixing between isotopically natural uranium and the isotopically depleted spike used in preparing the glasses. Laser ablation results match extremely well, generally within a few ppm, with solution analysis following sample dissolution and chemical separation. In addition to isotopic data, sample utilization efficiency measurements indicate that over 1% of ablated uranium atoms reach a mass spectrometer detector, making this technique extremely efficient. Laser sampling also allows for spatial analysis and our data indicate that rare uranium concentration inhomogeneities exist in NIST 616 glass.

1.1.5 Introduction

Femto-second laser ablation (fs-LA) sampling offers many advantages for analyzing solids including rapid sample analysis, high sample throughput, efficient aerosol transport, high spatial resolution, and the ability to ablate any material[1, 2]. Many recent publications utilize the advantages of fs-laser sampling for ultra-trace[3, 4], isotopic[5, 6], or elemental mapping applications[7, 8]. When coupled with a multicollector inductively coupled plasma mass spectrometer (MC-ICPMS) the two instruments offer outstanding sample utilization efficiency, high mass resolving power for interference reduction, and excellent element and isotope ratio measurements. Many of these advantages are exemplified in this investigation of the uranium isotopes of the NIST 61x glasses.

The NIST 61x (x=0,2,4,6) series of glasses were developed as multi-elemental standards that incorporate 61 elements at concentrations ranging from ~500 µg/g (NIST 610) to ~0.050 µg/g (NIST 616). These glasses are ubiquitously used in laser ablation as elemental and isotopic standards[9-12]. In fact, many publications and databases are committed to measuring and compiling the elemental content of the NIST glasses[13-19]. Most of the elements in the NIST 61x standards have natural isotopic composition[20]. Although the exact isotopic content varies slightly between glasses (due to isotopic differences between the spike and matrix glass), it typically falls within the accepted range of natural. In stark contrast to this trend, the elemental spike of uranium was isotopically depleted.

We (Duffin et al.)[21] recently published the first report of the full uranium isotopic composition of the NIST 61x series glasses, confirming the isotopic mixing between the depleted uranium spike and isotopically natural uranium in the bulk glass materials. Unfortunately, that study was hindered by a problematic polyatomic interference in the form of $PtAr^+$ ions and, at the time, the signal intensity was

too low for higher resolution analysis. However, recent improvements to the laser output energy allowed us to run similar experiment with the mass spectrometer in medium resolution mode, providing a means for mass separation of the true uranium signal from the $PtAr^+$ interference. The results indicate that the $PtAr^+$ interference in the previous experiment was insufficiently corrected. The aim of this study is to present results that are more accurate and much improved over the previous study.

In addition, this study aims to validate the laser ablation results with additional analysis by solution-based MC-ICPMS and solution-loaded thermal ionization mass spectroscopy (TIMS). Solutions of the uranium in NIST 61x glasses were made by dissolution followed by chemical separation. The sample dissolution and laser ablation results are in excellent agreement. Furthermore, Zimmer et al.[22] recently used a combination of ICPMS, thermal ionization mass spectroscopy, and secondary ionization mass spectroscopy to look at the uranium isotopes in NIST 610. Our results are consistent with their data for this glass and extend to the other three glasses in the series. However, the notes of the NIST certificates list literature values[23] as a guide for the uranium isotopic content of these glasses and in some cases these values are inconsistent with our results.

1.1.6 Experimental

A detailed description of the instruments was previously reported[18]. Briefly, the NeptunePlus mass spectrometer at the Pacific Northwest National Laboratory was purpose-built to measure uranium with detectors matched to the abundance of each isotope. Moreover, the major uranium isotopes can be switched between secondary electron multipliers (SEM) or Faraday cup (FC) detectors based on signal intensity. The femto-second laser ablation (fs-LA) system is model J-100 from Applied Spectra Inc. (Fremont, CA). Internally, the Ytterbium-doped gain medium of the S-pulse laser (Amplitude Systemes, Pessac, France) is directly pumped *via* laser diodes and produces <400 fs pulse at 1030 nm. This fundamental output (1 mJ/pulse) is frequency tripled to 343 nm for laser ablation work. Research has shown that pulse duration[24, 25] and wavelength[26, 27] are important parameters for fs-LA, but these parameters were fixed in the current studies. Pulse energy is controlled by rotating a half-wave plate placed between the laser head and the harmonic crystals, and the energy can be set from 0 to 100 µJ/pulse.

The ultra-short duration of an fs-laser pulse allows light to interact with a sample on a time scale shorter than many fundamental thermal processes[28-30]. More importantly for efficient ICPMS detection, the resulting aerosol has a particle size distribution that exhibits high transport efficiency from the ablation cell and high atomization/ionization in the plasma[30-33]. For the experiments described herein, the laser ablation aerosol is swept out of the ablation chamber with helium gas, typically at a flow rate of 0.6 L/min. The helium carrier gas is combined with Argon make-up gas and argon gas carrying aqueous aerosol. The aqueous aerosol is formed from a nebulized solution of dilute (2%) nitric acid or acid mixed with a uranium isotope standard. The isotope standards (solutions of CRM U010, U015, and 129-A) are used for detector cross-calibration and mass bias corrections. This setup is depicted in Fig. 1. The flow for the argon make-up gas is ca. 0.15 L/min, with the nebulizer stream contributing another ca. 0.85 L/min.

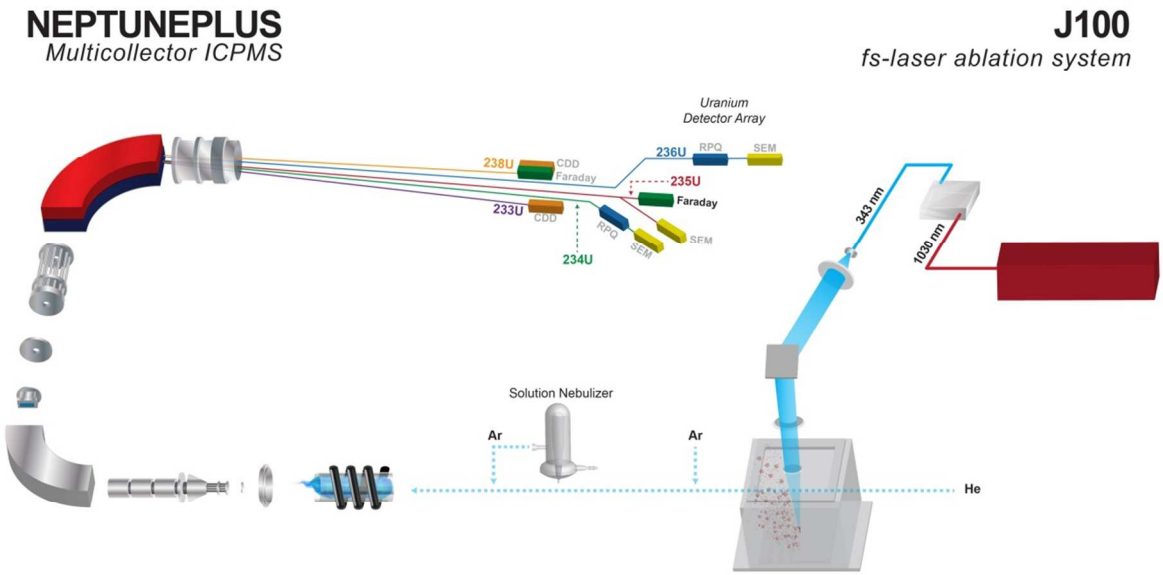

Fig. 1 Diagram of instrumental setup.

Laser ablation of the NIST standard reference material 61x (x=0,2,4,6) was performed by rastering the laser across the surface of the glass. Multiple wafers were rastered over many days to ensure sampling over wafer-to-wafer inhomogeneities. Each raster lasted ca. 30-60 seconds giving a pseudo-steady state signal during the ablation period. Laser ablation conditions were typically adjusted for each glass to keep the total uranium signal in a similar range for each glass. This necessitates orders-of-magnitude higher ablation rates for NIST 616 versus NIST 610, with intermediate ablation rates for 612 and 614. Table 1 lists typical ablation parameters for each glass. In practice, re-tuning plasma conditions after adjusting the scan speed, laser energy, and repetition rate for each glass was unnecessary as this procedure gave identical isotope ratio measurements at constant plasma settings. Initial experiments performed in low resolution mode revealed a large interference on top of the uranium signals from polyatomic $PtAr^+$ ions[21]. All subsequent experiments were performed with the NeptunePlus operating in medium or high resolution mode (resolving power of approximately 4000 or 10000 respectively). This mass resolution is sufficient to partially resolve most polyatomic interferences from the uranium ion signals (M/ΔM for U-PtAr ~2000). In addition, the uranium hydride signal was simultaneously monitored to make an internal hydride correction.

Table 1 fs-LA parameters for each NIST 61x glass.

fs-Laser Ablation Scan Parameters				
Glass	**Scan Speed (mm/sec)**	**Repetition Rate (Hz)**	**Energy/ Pulse (µJ)**	**Approx. Spot Size (µm)**
610	0.01	100	10	10
612	0.01	100	40	20
614	0.04	500	100	50
616	0.05	1000	100	50

Apart from laser ablation analysis, the NIST glass standards were dissolved and the solutions analyzed by MC-ICPMS. Great care was taken in maintaining sample integrity, all reagents were OPTIMA® grade, and labware was acid-leached prior to use. NIST glasses were first mechanically crushed and pulverized using a pre-cleaned mortar and pestle. The crushed material was transferred to acid-leached 22 mL Savillex® vials where repeated HF + HNO_3 treatments were performed until no visible grains of glass were identified. In most of the samples four treatments was sufficient, samples were dried on hot-plates at ~200 °C between treatments. Procedure blank samples were prepared in all cases. In the case of NIST 616, where approximately 2.6 g of sample was dissolved, several more treatments were required (a second reagent blank sample followed NIST 616). Following the HF + HNO_3 treatments all samples were subjected to aqua regia, nitric, and hydrochloric treatments (drying between each treatment on hot plates) until no visible salts remained.

Chemical purification of uranium was achieved by anion exchange. The anion exchange columns consisted of homemade columns loaded with 1mL of AG 1x4, 100-200 mesh. The samples were loaded in 6 M-HCl and washed with three column-volumes of 6 M-HCl followed by three column-volumes of 7.5 M-HNO_3. The columns utilized both HCl and HNO_3 with the intent of removing platinum, which has strong uptake on anion exchange resin in Cl^- form but does not adsorb to anion resin in NO_3^- form. Uranium was then eluted from the column with five column-volumes of 2% HNO_3. The resulting solutions were deposited on a carburized Re filament[34] and analyzed with a Triton (Thermo Scientific) TIMS instrument. Data acquisition was performed using a 4-step multi-static measurement scheme. Minor uranium isotopes (^{234}U, ^{236}U) were measured on the axial RPQ/SEM detector while contemporaneous detection of ^{238}U and ^{235}U were measured on FCs. All measurements were corrected for mass bias by externally correcting to isotopic standards (CRM-129a and U045) using an exponential mass bias law. Detector gain between the SEM and FC was determined in-run by measuring ^{235}U on both the SEM and FC detectors. The chemically separated uranium solutions were also analyzed using the NeptunePlus ICPMS. NIST glass solutions were run with the same detector configuration as the laser ablation experiments and in medium resolution mode to avoid any residual $PtAr^+$ interference. Detector gain and mass bias corrections were determined by standard-sample-standard bracketing using SRM 129A, U010, and U015. Uranium hydride corrections were made by concurrently monitoring mass 239 to get a first-order estimate of the UH^+/U^+ fraction.

Efficiency measurements were made by ablating craters in NIST 610, 612, and 614. Prior to crater production, the laser was rastered across the glass to allow for ICP adjustments to maximize signal from the individual glasses. For each glass, five craters were made at each of five different laser energies. Ten laser pulses were used for each crater. During crater production, the ^{238}U signal was monitored and integrated to obtain the number of ions reaching the detector. Afterwards, the crater volumes were measured *via* white light interferometry (Zygo NewView 600). With the known (certificate) concentration of uranium in each of the glasses, the crater volume was used to calculate the number of uranium atoms ablated and an overall efficiency (ions detected relative to atoms ablated).

The isotopic ratio equations used in our spike isotopic calculation are given by

$$\frac{M_s^{(i)} C_s I_{s,j} + M_g^{(i)} C_g I_{g,j}}{M_s^{(i)} C_s I_{s,238} + M_g^{(i)} C_g I_{g,238}} = \frac{{}^{j}\mathrm{U}^{(i)}}{{}^{238}\mathrm{U}^{(i)}},$$

for glass $i = 610,612,614,616$ and isotope $j = 236,235,234$, where M is mass, C is concentration, I is isotope atom percent, and subscripts g and s indicate matrix glass and spike, respectively. The ratio on

the right represents a measured value (or the mean values as reported in Table 1). The concentration equations are

$$\frac{M_s^{(i)} C_s + M_g^{(i)} C_g}{M_s^{(i)} + M_g^{(i)}} = K^{(i)},$$

where K is measured total uranium concentration value, with one value for each glass. Using the fact that $\sum_{j=1}^{4} I_{s,j} = 1$ and re-arranging equations, we obtained a set of 16 equations, linear in the combined variables $C_s I_{s,2}, C_s I_{s,3}, C_s I_{s,4}, C_s$, and C_g. We then obtained a least-squares solution of the system for the spike isotopic values.

To estimate the error, we used Monte Carlo simulation assuming normally distributed error in the measured isotopic ratios, measured total uranium concentrations, and spike and matrix glass masses, resampling each of these values 100,000 times to obtain an ensemble of 100,000 solutions. The mean and error of the isotopic ratios were obtained from fs-LA data (presented below). The remaining values and associated error are listed in Table 2.

Table 2 Values and error utilized in the Monte Carlo simulations to estimate the error associated with the calculation of the spike uranium isotopics.

	Monte Carlo Simulation Input Parameters[1]		
Glass	Matrix Mass[2] (kg)	Spike Mass[2] (kg)	Total U Conc.[3] (ppm)
610	97.0±0.1	3.05±0.01	461.5±1.1
612	99.7±0.1	0.305±0.001	37.38±0.08
614	100.0±0.1	0.0061±0.0001	0.823±0.002
616	100.0±0.1	0.000122±0.000001	0.0721±0.0013

[1] Isotopic ratio estimates were obtained from the fs-LA data in Table 4.

[2] Mass error estimates were not listed in Kane et al.; a nominal value is used based on the assumption that listed values were roughly within one unit of the last significant digit.

[3] Total uranium concentration error estimates were based on NIST certificates.

1.1.7 Results and discussion

High spatial resolution is one advantage of fs-LA-MC-ICPMS. Previous results showed obvious inhomogeneity in the Pt distribution of NIST 61x glasses, a result of melting crucible contamination.[18] In the current experiments, the spatial resolution and mass resolving power of the fs-LA-MC-ICPMS system allowed for the identification of rare, but unmistakable, uranium inhomogeneities. Fig. 2 is a waterfall plot of 15 parallel lines rastered over a 3 x ~1.5 mm area of NIST 616, showing a definite increase in uranium concentration near the center of the rastered area. The isotopics of this inclusion match natural uranium ($^{235}U/^{238}U$ =0.007±0.002), but the poor isotopic precision of the inhomogeneity does not preclude it from being NIST 616. It is unlikely that the inhomogeneity was surface contamination, as it persisted for repeated raster lines. It is also unlikely that it is unmixed bulk glass material, as the uranium concentration of the matrix glass is less than the uranium concentration of NIST 616. Due to the ca. 2 sec washout time of the sample chamber, the inhomogeneity in Fig. 2 can only be assigned an

upper limit in size. That is, the inhomogeneity cannot be larger than 100x100 μm^2. The rarity of these uranium inhomogeneities precluded any statistical conclusion on the spatial distribution of uranium in NIST 616.

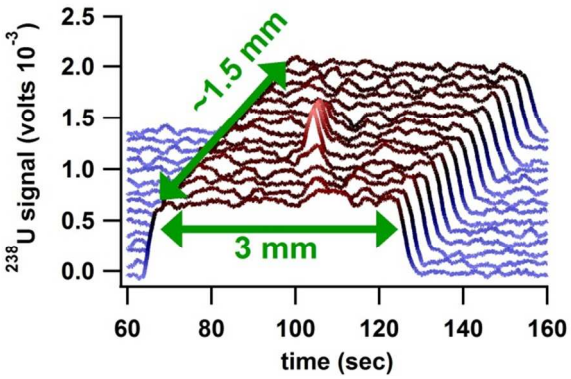

Fig. 2 Area raster of NIST 616 glass showing a uranium concentration inhomogeneity.

The detection of a small concentration inhomogeneity in the NIST 616 glass is aided by the excellent sample utilization efficiency of the fs-LA-MC-ICPMS system. Fig. 3 shows the detection efficiency (atoms detected over atoms ablated) for uranium as a function of pulse energy and for three different NIST glasses. The large spread in the data precludes the detection of subtle trends, but it is clear that the average sample utilization efficiency is ca. 1.5% and that this number does not vary significantly with laser energy or glass. A sample utilization efficiency of 1.5% is excellent for laser ablation analysis and is a result of the high transport efficiency of fs-ablation aerosol in combination with the excellent efficiency of the NeptunePlus. This number indicates that fs-LA-MC-ICPMS can be used for very sensitive uranium analysis. It also compares favorably with other mass spectrometric techniques, notably TIMS and secondary ion mass spectroscopy (SIMS), which each report efficiencies of about 1% for uranium[35, 36]. This efficiency applies only to operation in low resolution mode; in medium and high resolution modes the transmission of the NeptunePlus decreases by 71% and 87%, respectively.

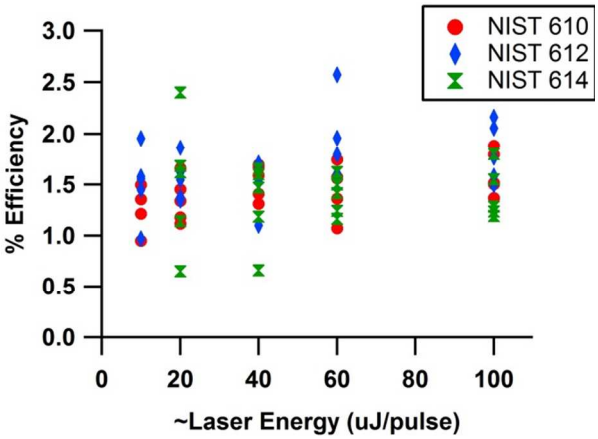

Fig. 3 Efficiency of atoms detected to atoms ablated as a function of laser energy and for three NIST 61x glasses.

Fig. 4 plots the isotopic data from each individual raster of the NIST glasses on a dual three-isotope plot (both $^{234}U/^{238}U$ and $^{236}U/^{238}U$ are plotted against $^{235}U/^{238}U$). The linear behavior observed indicates a simple mixing of the depleted uranium spike with isotopically natural uranium in the bulk glass material. From NIST 610 to 616, the spike became more dilute in the bulk glass and the isotopic values of the glass moved toward natural uranium. The dashed lines in Fig. 4 show isotopic mixing from the measured value for the depleted uranium spike in NIST 610 and natural uranium (54ppm ^{234}U, 0ppm ^{236}U, and 7204 ppm ^{235}U). Within uncertainty, the fs-LA-MC-ICPMS data fall on this mixing line. The data clouds in Fig. 4 are also reasonably symmetric, without any skew along $PtAr^+$ mixing lines observed in previous, low resolution experiments[21]. Atom percent data measured by fs-LA-MC-ICPMS is given in Table 3. The data in Table 3 show that the ^{235}U values measured by fs-LA-MC-ICPMS are not wholly consistent with the values listed in the certificate notes.

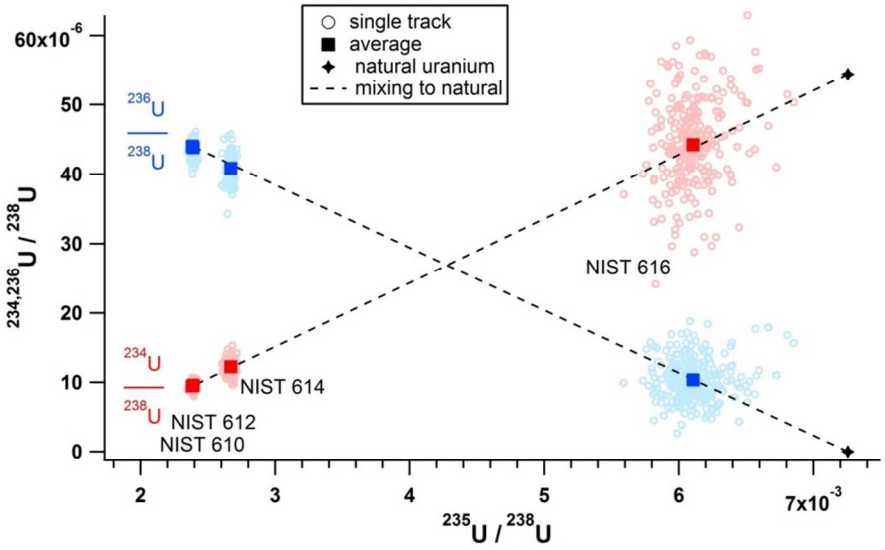

Fig. 4 Three-isotope plot showing individual raster data and averages for each of the NIST 61x glasses. The dashed lines show expected mixing lines from the values measured for NIST 610 and natural uranium. At the plotted scale, the NIST 610 and NIST 612 lie on top of each other.

Table 3 Uranium isotope atom percent values (± 2σ or 95% CI) for NIST 61x glasses measured via fs-LA-MC-ICPMS. Published or Certificate values when available are shown in parentheses. Percent differences between the present study and published/certificate values are shown in square brackets.

Uranium Isotope Atom Percent in NIST 61x Glass *via* fs-LA-MC-ICPMS

Glass	^{238}U	^{236}U	^{235}U	^{234}U
610	99.7569±0.0001 (99.7571) [-0.0002]	0.004393 ±0.000007 (0.0043) [2.2]	0.2378 ±0.0001 (0.2376) [0.08]	0.000946 ±0.000003 (0.0010) [-5.4]
612	99.7562 ±0.0001	0.004370 ±0.000013	0.2385 ±0.0001 (0.2392) [-0.3]	0.000954 ±0.000004
614	99.7284 ±0.0003	0.00407 ±0.00002	0.2663 ±0.0003 (0.2792) [-4.6]	0.00122 ±0.00001
616	99.388 ±0.002	0.00103 ±0.00003	0.607 ±0.002 (0.616) [-1.5]	0.00440 ±0.00006

value ± 2σ (published or certificate value) [percent difference]

To help resolve the discrepancy between the certificate note values and the values measured by fs-LA-MC-ICPMS, the glasses were dissolved, the uranium extracted, and the resulting solution measured by traditional solution nebulization on the NeptunePlus multicollector and with solution-loaded multicollector TIMS. A second dissolution and extraction was performed on NIST 612, 614, and 616, and the uranium isotopic ratios were measured with TIMS only.

The NIST glass solution data, the average fs-LA results, and the certificate values are all plotted in Fig. 5 with values from this work printed in Table 4. Inserts in Fig. 5 show expanded views around the individual glasses. The lower uncertainty for the fs-LA results compared to the TIMS and solution-based MC-ICPMS results is likely an artifact of the number of averaged measurements. Laser ablation offers the advantage of rapidly collecting many data sets, and the fs-LA data are a compilation of hundreds of raster scans collected over many days while the TIMS results are from a limited number of measurements. However, each technique analyzed a similar total mass of uranium (tens to hundreds of nanograms). Additional efforts to resolve the discrepancy between laser ablation and solution values included direct TIMS and SIMS analysis of NIST glass shards. The former failed to produce a useful ion yield (for either U^+ or UO^+) and the latter, run on a Cameca 4f, was unable to separate out interfering molecular species. However, Zimmer et al.[22] recently measured the uranium $^{235}U/^{238}U$ isotope ratio in NIST 610/611 with a 1280 SIMS instrument. Their measured value of 0.00238±0.00004 is easily consistent with the ratios measured in this study.

Table 4 Comparison of isotope ratio values (in parts-per-million) as measured by fs-LA-MC-ICPMS, MC-ICPMS, and TIMS. (2σ uncertainty).

Uranium Isotope Ratios NIST 61x Glass

Glass	Technique	Measurements	$^{234}U/^{238}U$ (ppm)	$^{235}U/^{238}U$ (ppm)	$^{236}U/^{238}U$ (ppm)
610	fs-LA	n=127	9.48±0.03	2384±1	44.04±0.07
	MC-ICPMS (sol #1)	1	9.26±0.13	2381±3	43.53±0.46
	TIMS (sol #1)	3	9.32±0.05	2387±3	43.55±0.16
	TIMS (sol #2)		–	–	–
612	fs-LA	129	9.56±0.04	2390±1	43.8±0.1
	MC-ICPMS (sol #1)	1	9.36±0.12	2393±2	43.4±0.4
	TIMS (sol #1)	3	9.35±0.04	2392±3	43.4±0.2
	TIMS (sol #2)	4	9.40±0.02	2397±2	43.5±0.1
614	fs-LA	165	12.2±0.1	2670±3	40.8±0.2
	MC-ICPMS (sol #1)	1	12.3±0.2	2721±3	40.4±0.6
	TIMS (sol #1)	1	12.4±0.1	2724±15	40.6±0.3
	TIMS (sol #2)	3	12.2±0.2	2690±13	40.9±0.6
616	fs-LA	260	44.2±0.6	6106±19	10.3±0.3
	MC-ICPMS (sol #1)	1	45.1±0.6	6130±9	10.5±0.3
	TIMS (sol #1)	1	43.1±1.4	6118±38	09.3±0.7
	TIMS (sol #2)	3	41.1±6.9	6115±56	09.3±2.7

For NIST 616, recently collected isotopic data are in agreement and falls on the isotopic mixing line to natural uranium. In this case the glass dissolution results confirm the laser ablation analysis and both appear inconsistent with the certificate note value. (Without uncertainty on the certificate note values, it is impossible to definitively conclude that the measurements are incongruous.) However, given the consistency of the recent data, it is likely that the laser ablation values reported here are excellent measurements of the true uranium isotopics of NIST 616.

NIST 614 is a different case than NIST 616. Of the two NIST 614 dissolutions, only one is consistent with the laser ablation value. It is possible that the first dissolution became contaminated with natural uranium and thus moved the measurements up the isotopic mixing line. Even though the two dissolution measurements do not agree, it is clear from Fig. 5 that recent data are significantly different than the certificate note value.

For the major isotopes, the laser ablation results for NIST 610 and 612 are consistent with the solution results. However, laser ablation gives slightly higher values for the $^{234}U/^{238}U$ and $^{236}U/^{238}U$ (See Table 4) isotopic ratios than measured *via* solution introduction. A possible reason for this offset is unknown interferences from the complicated NIST glass matrix. For example, $PbSi^+$, for example would interfere with the minor uranium isotopes and requires a higher resolving power than $PtAr^+$, 2600 and 2000 respectively, to separate from uranium. These interferences would have been removed in the uranium

extraction step of the solution preparation, hence the lower $^{234}U/^{238}U$ and $^{236}U/^{238}U$ ratios with solution introduction. However, Zimmer et al. also dissolved NIST 611 and isolated the uranium for measurement by MC-ICPMS and MC-TIMS. Their results (averaged with the results from Stirling et al.[12]) are also plotted in Fig. 5 and are entirely consistent with our laser ablation results.

The isotopic analysis of NIST 61x glasses highlights both the advantages and disadvantages of LA-MC-ICMPS. Even without any sample preparation, laser ablation was able to measure uranium isotope ratios on par with the more time-consuming dissolution and chemical separation techniques. In other words, this technique offers rapid analysis without sacrificing accuracy or precision. Moreover, TIMS was only able to obtain results for chemically separated solution, not for direct analysis of the glass. The same is true for SIMS where the complex matrix presented too many interferences for a small-format SIMS instrument to reliably measure the uranium isotopics. Zimmer et al. were able to measure the uranium isotopics with a large-format SIMS instrument, but only for NIST 610 and with much lower precision. Thus, fs-LA in conjunction with MC-ICPMS provides a powerful tool for rapidly analyzing uranium in complex matricies. However, the lack of chemical separations presumably led to interferences that may have shifted the accuracy of the final laser ablation results, albeit in the seventh decimal place; compare ca. 9.3 to 9.5 ppm respectively for the NIST 610 solution and laser ablation measured $^{234}U/^{238}U$ isotope ratio.

The isotope ratio results also allow us to tease out additional details regarding the original glass preparation. Using existing specifications for the relative masses of spike and matrix glass, such as those detailed in Table 1 of Kane[18], one can estimate the spike uranium isotopics. Due to the overwhelming contribution of spike uranium to matrix glass uranium, the spike isotopics are expected to be nearly identical to the measured values for NIST 610. The calculation involves a set of equations that link spike and matrix masses, uranium concentrations, and isotopics to measured total isotopic ratios, and equations that link masses and uranium concentrations to measured total uranium concentration. This leads to an over-determined linear system of equations that, in principle, admits a simple least-squares solution. However, using the masses listed in Kane's table[18] produces non-physical results; our calculations suggest that one of the masses in Kane's table was specified incorrectly. Specifically, for NIST 616, using a spike mass of 0.122 grams (added to 100 kg matrix) rather than the reported 1.22 grams in our calculation produces spike uranium isotopics very close to those of NIST 610 (see Table 1) as expected: approximately 99.763±0.004%, 0.00441±0.00004%, 0.232±0.004%, and 0.00093±0.00008% for ^{238}U, ^{236}U, ^{235}U, and ^{234}U, respectively (±2σ). The NIST 610 measured values are within the estimated error bounds. These calculations also reveal that that the 61 element spike used to make these glasses was 1.33±0.01% uranium by mass and the matrix glass contained 55.8±0.1 ng/g of natural uranium.

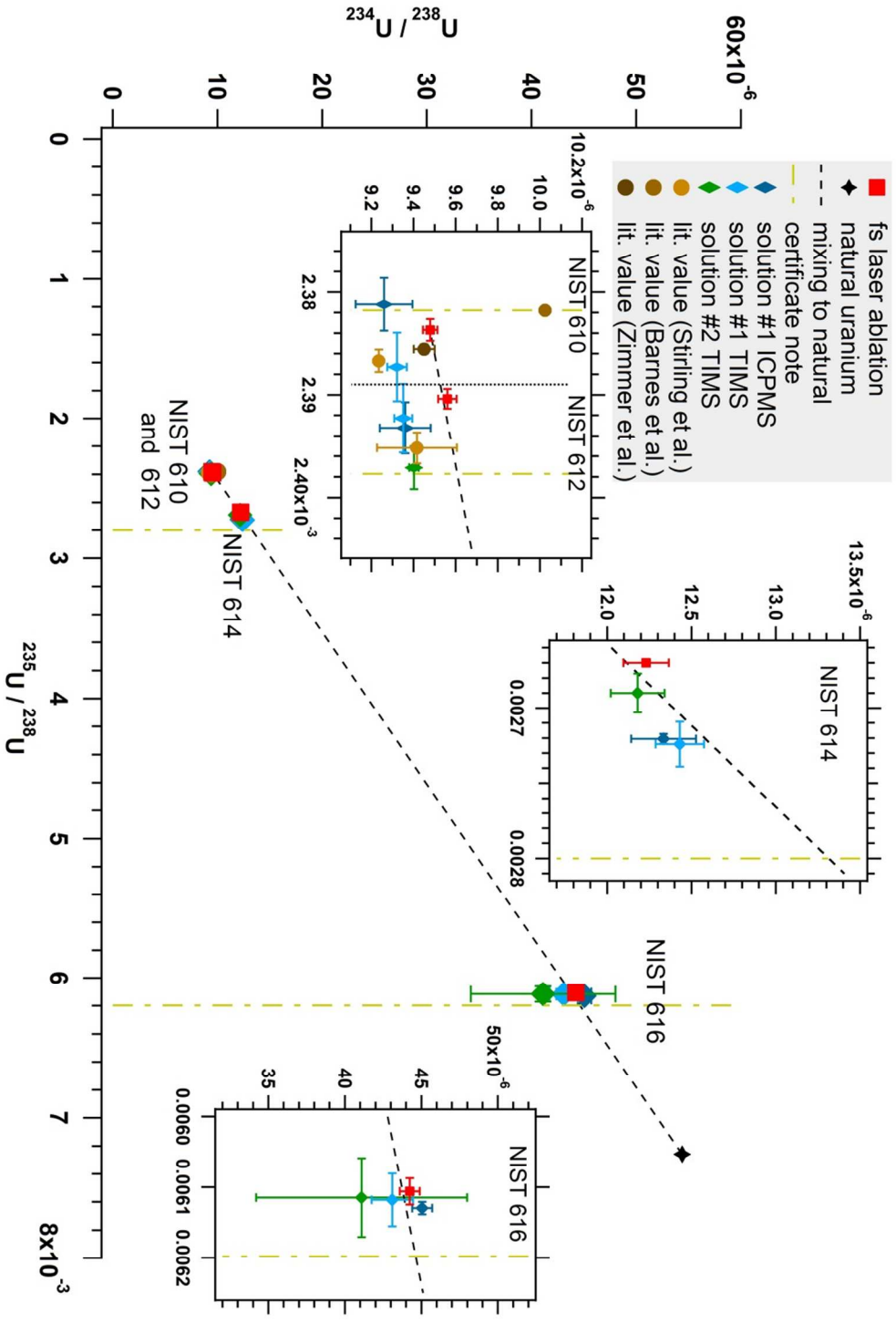

Fig. 5 Three-isotope plot of fs-LA data for $^{234}U/^{238}U$ vs $^{235}U/^{238}U$, glass dissolution data, and certificate values for the uranium in NIST 61x glass. The inset graphs are expanded views around each glass. Error bars are +/- 2σ sigma.

1.1.8 Conclusion

Fs-LA-MC-ICPMS has proven to be a highly efficient technique for rapid isotopic analysis of uranium-bearing solids. The high mass resolution of the NeptunePlus multicollector allows for effective separation of the uranium ions of interest and molecular interferences, $PtAr^+$ in this particular case. New values for the uranium isotopes in NIST 61x glasses have been presented. Isotopic measurements made on dissolved glass samples match the fs-LA results but neither are entirely consistent with the previous literature values reported in the NIST certificate notes. This analysis highlights the ability of fs-LA-MC-IPCMS to serve as a useful nuclear forensics tool.

1.1.9 Acknowledgements

The National Nuclear Security Administration, Office of Defense Nuclear Nonproliferation Research and Engineering, DNN-RD/NA-22, supported this work under an Interagency Agreement with the U.S. Department of Energy (DOE) under Contract DE-AC05-75RLO1830. Part of this work was supported by the Chemical Science Division, Office of Basic Energy Sciences and the Defense Nuclear Nonproliferation Research and Development Office of the U.S. DOE under contract number DE-AC02-05CH11231 at the Lawrence Berkeley National Laboratory.

1.1.10 Dedications

1.1.11 Bibliographic references and notes

1 J. Koch and D. Gunther, *Appl. Spectrosc.*, 2011, **65**, 155A-162A. DOI: 10.1366/11-06255.

2 R. E. Russo, X. L. Mao, J. J. Gonzalez, V. Zorba and J. Yoo, *Analytical Chemistry*, 2013, **85**, 6162-6177. DOI: 10.1021/ac4005327.

3 D. S. Macholdt, K. P. Jochum, B. Stoll, U. Weis and M. O. Andreae, *Chem. Geol.*, 2014, **383**, 123-131. DOI: 10.1016/j.chemgeo.2014.06.001.

4 A. Hubert, F. Claverie, C. Pecheyran and F. Pointurier, *Spectrochimica Acta Part B-Atomic Spectroscopy*, 2014, **93**, 52-60. DOI: 10.1016/j.sab.2013.12.007.

5 J. A. Schuessler and F. von Blanckenburg, *Spectrochimica Acta Part B: Atomic Spectroscopy*, 2014, **98**, 1-18. DOI: http://dx.doi.org/10.1016/j.sab.2014.05.002.

6 L. Dorta, R. Kovacs, J. Koch, K. Nishiguchi, K. Utani and D. Gunther, *Journal of Analytical Atomic Spectrometry*, 2013, **28**, 1513-1521. DOI: 10.1039/c3ja50126d.

7 M. Bonta, H. Lohninger, M. Marchetti-Deschmann and A. Limbeck, *Analyst*, 2014, **139**, 1521-1531. DOI: Doi 10.1039/C3an01511d.

8 H. A. O. Wang, D. Grolimund, C. Giesen, C. N. Borca, J. R. H. Shaw-Stewart, B. Bodenmiller and D. Günther, *Analytical Chemistry*, 2013, **85**, 10107-10116. DOI: 10.1021/ac400996x.

9 Z. Varga, *Anal. Chim. Acta*, 2008, **625**, 1-7. DOI: 10.1016/j.aca.2008.07.012.

10 F. Pointurier, A. C. Pottin, P. Hemet and A. Hubert, *Spectrochimica Acta Part B-Atomic Spectroscopy*, 2011, **66**, 261-267. DOI: 10.1016/j.sab.2011.03.003.

11 J. S. Becker, C. Pickhardt and H. J. Dietze, *Mikrochim. Acta*, 2000, **135**, 71-80. DOI: 10.1007/s006040070020.

12 C. H. Stirling, D. C. Lee, J. N. Christensen and A. N. Halliday, *Geochimica Et Cosmochimica Acta*, 2000, **64**, 3737-3750. DOI: 10.1016/s0016-7037(00)00457-9.

13 S. M. Eggins and J. M. G. Shelley, *Geostandards Newsletter-the Journal of Geostandards and Geoanalysis*, 2002, **26**, 269-286. DOI: 10.1111/j.1751-908X.2002.tb00634.x.

14 K. P. Jochum, L. Nohl, K. Herwig, E. Lammel, B. Toll and A. W. Hofmann, *Geostand. Geoanal. Res.*, 2005, **29**, 333-338. DOI: 10.1111/j.1751-908X.2005.tb00904.x.

15 K. P. Jochum, U. Weis, B. Stoll, D. Kuzmin, Q. C. Yang, I. Raczek, D. E. Jacob, A. Stracke, K. Birbaum, D. A. Frick, D. Gunther and J. Enzweiler, *Geostand. Geoanal. Res.*, 2011, **35**, 397-429. DOI: 10.1111/j.1751-908X.2011.00120.x.

16 J. S. Kane, *Geostandards Newsletter-the Journal of Geostandards and Geoanalysis*, 1998, **22**, 15-31. DOI: 10.1111/j.1751-908X.1998.tb00542.x.

17 N. J. G. Pearce, W. T. Perkins, J. A. Westgate, M. P. Gorton, S. E. Jackson, C. R. Neal and S. P. Chenery, *Geostandards Newsletter-the Journal of Geostandards and Geoanalysis*, 1997, **21**, 115-144. DOI: 10.1111/j.1751-908X.1997.tb00538.x.

18 J. S. Kane, *Geostandards Newsletter-the Journal of Geostandards and Geoanalysis*, 1998, **22**, 7-13. DOI: 10.1111/j.1751-908X.1998.tb00541.x.

19 I. Horn, R. W. Hinton, S. E. Jackson and H. P. Longerich, *Geostandards Newsletter-the Journal of Geostandards and Geoanalysis*, 1997, **21**, 191-203. DOI: 10.1111/j.1751-908X.1997.tb00670.x.

20 J. D. Woodhead and J. M. Hergt, *Geostandards Newsletter*, 2001, **25**, 261-266. DOI: 10.1111/j.1751-908X.2001.tb00601.x.

21 A. M. Duffin, G. L. Hart, R. C. Hanlen and G. C. Eiden, *Journal of Radioanalytical and Nuclear Chemistry*, 2013, **296**, 1031-1036. DOI: 10.1007/s10967-012-2218-8.

22 M. M. Zimmer, W. S. Kinman, A. H. Kara and R. E. Steiner, *Minerals*, 2014, **4**, 541-552. DOI: 10.3390/min4020541.

23 I. L. Barnes, E. L. Garner, J. W. Gramlich, L. J. Moore, T. J. Murphy, L. A. Machlan, W. R. Shields, Tatsumot.M and R. J. Knight, *Analytical Chemistry*, 1973, **45**, 880-885. DOI: 10.1021/ac60328a005.

24 N. L. LaHaye, S. S. Harilal, P. K. Diwakar and A. Hassanein, *Journal of Analytical Atomic Spectrometry*, 2013, **28**, 1781-1787. DOI: 10.1039/c3ja50200g.

25 F.-X. d'Abzac, A.-M. Seydoux-Guillaume, J. Chmeleff, L. Datas and F. Poitrasson, *Spectrochimica Acta Part B: Atomic Spectroscopy*, 2011, **66**, 671-680. DOI: http://dx.doi.org/10.1016/j.sab.2011.09.010.

26 M. Ohata, D. Tabersky, R. Glaus, J. Koch, B. Hattendorf and D. Gunther, *Journal of Analytical Atomic Spectrometry*, 2014, **29**, 1345-1353. DOI: 10.1039/c4ja00030g.

27 N. L. LaHaye, S. S. Harilal, P. K. Diwakar, A. Hassanein and P. Kulkarni, *J. Appl. Phys.*, 2013, **114**, 10. DOI: 10.1063/1.4812491.

28 R. Hergenroder, O. Samek and V. Hommes, *Mass Spectrom. Rev.*, 2006, **25**, 551-572. DOI: 10.1002/mas.20077.

29 R. E. Russo, X. L. Mao, J. H. Yoo and J. J. Gonzalez, in *Laser-Induced Breakdown Spectroscopy*, ed. P. S. Jagdish and N. T. Surya, Elsevier, Amsterdam. 2007, pp. 49-82.

30 B. Fernandez, F. Claverie, C. Pecheyran and O. F. X. Donard, *Trac-Trends Anal. Chem.*, 2007, **26**, 951-966. DOI: 10.1016/j.trac.2007.08.008.

31 F. X. D'Abzac, A. M. Seydoux-Guillaume, J. Chmeleff, L. Datas and F. Poitrasson, *Journal of Analytical Atomic Spectrometry*, 2012, **27**, 108-119. DOI: 10.1039/c1ja10154d.

32 I. Horn and D. Gunther, *Appl. Surf. Sci.*, 2003, **207**, 144-157. DOI: 10.1016/s0169-4332(02)01324-7.

33 C. C. Garcia, M. Waelle, H. Lindner, J. Koch, K. Niemax and D. Guenther, *Spectrochimica Acta Part B-Atomic Spectroscopy*, 2008, **63**, 271-276. DOI: 10.1016/j.sab.2007.11.017.

34 J. M. Kelley and D. M. Robertson, *Analytical Chemistry*, 1985, **57**, 124-130. DOI: 10.1021/ac00279a033.

35 Y. Ranebo, P. M. L. Hedberg, M. J. Whitehouse, K. Ingeneri and S. Littmann, *Journal of Analytical Atomic Spectrometry*, 2009, **24**, 277-287. DOI: 10.1039/b810474c.

36 J. J. Stoffels, J. K. Briant and D. S. Simons, *J Am Soc Mass Spectr*, 1994, **5**, 852-858. DOI: Doi 10.1016/1044-0305(94)87008-X.